A project dissertation on

THERMAL NEUTRON IRRADIATION STUDIES ON STRUCTURAL, OPTICAL AND ELECTRICALPROPERTIES OF n-TYPE 4H-SiC

Submitted to

ಬೆಂಗಳೂರು ನಗರ ವಿಶ್ವವಿದ್ಯಾಲಯ BENGALURU CITY UNIVERSITY

BE BOUNDLESS

in partial fulfilment of the requirements for the award of the Degree of

Master of Science

(Physics)

Submitted by

Divyashree Gowda K L (Reg. No. : PH190201)

Komaladevi A V (Reg. No. : PH190202)

Lakshmi P (Reg. No. : PH190203)

Madhushree K (Reg. No. : PH190204)

Under the guidance of

Dr. Indudhar P. Vali

Assistant Professor

Department of Physics (PG)

K. L. E. Society's S. Nijalingappa College

Bengaluru – 560010, Karnataka, India

2020

CERTIFICATE FROM THE PROJECT GUIDE

This is to certify that the work incorporated in this project dissertation based on secondary data, is in consideration of UGC guidelines due to ongoing COVID-19 crisis. The title of research work is "THERMAL NEUTRON IRRADIATION STUDIES ON STRUCTURAL, OPTICAL AND ELECTRICALPROPERTIES OF n-TYPE 4H-SiC" submitted by Divyashree Gowda K L (Reg. No. : PH190201), Komaladevi A V (Reg. No. : PH190202), Lakshmi P (Reg. No. : PH190203) and Madhushree K (Reg. No. : PH190204) was carried out under my guidance.

Dr. Indudhar P. Vali
Research Project Guide
Assistant Professor
Department of Physics (PG)
K. L. E. Society's S. Nijalingappa College
Bengaluru – 560010, Karnataka, India.

2020

CERTIFICATE FROM THE HEAD OF THE DEPARTMENT

This is to certify that the work incorporated in this project dissertation based on secondary data, is in consideration of UGC guidelines due to ongoing COVID-19 crisis. The title of research work is “THERMAL NEUTRON IRRADIATION STUDIES ON STRUCTURAL, OPTICAL AND ELECTRICALPROPERTIES OF n-TYPE 4H-SiC” submitted by Divyashree Gowda K L (Reg. No. : PH190201), Komaladevi A V (Reg. No. : PH190202), Lakshmi P (Reg. No. : PH190203) and Madhushree K (Reg. No. : PH190204) was carried out under the guidance of Dr. Indudhar P. Vali, Assistant Professor, Department of Physics (PG), K. L. E. Society’s S. Nijalingappa College, Bengaluru – 560010, Karnataka, India.

Head of the Department

2020

ಬೆಂಗಳೂರು ನಗರ ವಿಶ್ವವಿದ್ಯಾಲಯ BENGALURU CITY UNIVERSITY

BE BOUNDLESS

CERTIFICATE FROM THE HEAD OF THE INSTITUTION

This is to certify that the work incorporated in this project dissertation based on secondary data, is in consideration of UGC guidelines due to ongoing COVID-19 crisis. The title of research work is "THERMAL NEUTRON IRRADIATION STUDIES ON STRUCTURAL, OPTICAL AND ELECTRICALPROPERTIES OF n-TYPE 4H-SiC" submitted by Divyashree Gowda K L (Reg. No. : PH190201), Komaladevi A V (Reg. No. : PH190202), Lakshmi P (Reg. No. : PH190203) and Madhushree K (Reg. No. : PH190204) was carried out under the guidance of Dr. Indudhar P. Vali, Assistant Professor, Department of Physics (PG), K. L. E. Society's S. Nijalingappa College, Bengaluru – 560010, Karnataka, India.

Principal

DECLARATION BY CANDIDATES

We declare that the project dissertation, submitted for the degree of Master of Science (Physics) to Bengaluru City University, is a research work based on secondary data in consideration of UGC guidelines due to ongoing COVID-19 crisis. The research project entitled "THERMAL NEUTRON IRRADIATION STUDIES ON STRUCTURAL, OPTICAL AND ELECTRICALPROPERTIES OF n-TYPE 4H-SiC" is conducted under the supervision of our guide Dr. Indudhar P. Vali, Assistant Professor, K.L.E. Society's S. Nijalingappa College, Bengaluru, India. We also wish to inform that no part of the research has been submitted for a degree or examination at any university. References, help and material obtained from other sources have been duly acknowledged.

Divyashree Gowda K L (Reg. No. : PH190201)
Komaladevi A V (Reg. No. : PH190202)
Lakshmi P (Reg. No. : PH190203)
Madhushree K (Reg. No. : PH190204)

2020

ACKOWLEDGEMENTS

With great pleasure, we take this opportunity to express our deep sense of gratitude and heart-felt thanks to several individuals, whom received impetus and motivation during the course of our project work. We extend our thanks to our guide Dr. Indudhar P. Vali, Assistant Professor, Department of Physics for his encouragement, valuable suggestion and guidance in completing our project work.

We wish to thank faculties of our department Dr. Shivananda C. S, Mr. Vishal S. V, and our department head, Prof. K. Nagi Reddy, for their valuable suggestions and kind co-operation throughout the MSc course. We extend our gratitude to non-teaching staff Mr. Dayananda Murthy K. S. for his support. Also, we extend thanks to our Principal Dr. Arunkumar B. Sonappanavar for his constant encouragement and support throughout our project work. We thank our friends who helped us in completing this project work.

We are grateful to our beloved parents who had been constant source of inspiration and moral support throughout our studies.

Divyashree Gowda K L

Komaladevi A V

Lakshmi P

Madhushree K

2020

Abstract

In the past two decades silicon carbide (SiC) has gained much importance in the field of devices operating in high-temperature, high-power and radiation environments. However, the exposure of SiC-based devices or any other material and devices in the radiation environments are always interesting to explore. Since radiation induced effects on the samples depends on several radiation parameters such as type of radiation, energy, flux and exposure time. In the present work, the thermal neutron irradiation effects on the structural and optical properties of n-4H–SiC, and electrical properties of Al/n-4H–SiC Schottky contacts is detailed. The noticeable modifications observed in the irradiated samples were studied by using different techniques. The X-ray diffraction studies revealed a decrease in the lattice parameter of the irradiated samples due to isotopic modifications and irradiation-induced defects in the material. As a result, the energy bandgap, Urbach energy, longitudinal optical phonon–plasmon coupling mode, free carrier concentration, defect related photoluminescence and nitrogen bound exciton photoluminescence bands were prominently affected in the irradiated samples. The current–voltage characteristics of neutron irradiated Al/n-4H–SiC Schottky contacts were also strikingly affected in terms of zero-bias offset as well as decrease in the forward current. These modifications along with the increase in the Schottky junction parameters (such as ideality factor and Schottky barrier height) were mainly attributed neutron-induced isotopic effects as well as decrease in the free carrier concentration due to neutron-induced defect states.

Contents

Chapter 1: Introduction			1-13
	1.1.	Silicon Carbide	1
	1.2.	Interaction of neutrons with matter	4
	1.3.	Schottky Contacts	6
		1.3.1. Formation of Schottky Barrier	8
		1.3.2. Current-Voltage Characteristics of Schottky contacts	11
Chapter 2: Literature Review			14-16
	2.1.	Radiation Effects on 4H-SiC Schottky Contacts	14
	2.2.	Research Objectives	16
Chapter 3: Experimental Techniques and Methodology			17-22
	3.1.	Materials	17
	3.2.	Schottky Contact Fabrication	17
	3.3.	Neutron Radiation Source	18
	3.4.	Characterization Techniques	18
		3.4.1. X–ray diffraction (XRD)	18
		3.4.2. Raman spectroscopy (RS)	20
		3.4.3. UV–Visible absorption spectroscopy	20
		3.4.4. Photoluminescence spectroscopy (PLS)	21
		3.4.5. Current–voltage (I–V) Characterisation	22
Chapter 4: Results and Discussion			23-31
	4.1.	XRD analysis	23
	4.2.	UV–Vis absorption spectra analysis	25
	4.3.	Raman spectra analysis	26
	4.4.	PL spectra analysis	27
	4.5.	Electrical studies on Al/n–4H–SiC Schottky contacts	28
Chapter 5: Conclusion and Future Work			32-33
	5.1.	Conclusion	32
	5.2.	Future Work	32
References			34–37

Chapter 1

Introduction

1.1.Silicon Carbide

Silicon carbide (SiC) is an important $Si-$ and $C-$based, nontoxic, covalent, wide bandgap ($\sim$3.3 eV) semiconductor material. The availability of single crystal SiC wafers during 1990s have initiated the development of $SiC-$based devices. Soon the commercial blue light emitting diodes (LEDs) were realised from this material. Due to superior physical properties and matured technology of SiC, it has drawn much attention in the development of potential device applications in the field of high–temperature, high–frequency, high–power and high–radiation environments [1, 2].

Table 1.1. Basic physical properties of well–known semiconductors [Ref. 1].

	Si	GaAs	4H–SiC	GaN	Diamond
Energy bandgap (eV)	1.12	1.43	3.3	3.4	5.5
Electron mobility ($cm^2V^{-1}s^{-1}$)	1450	8600	980	2000	4000
Hole mobility ($cm^2V^{-1}s^{-1}$)	480	400	200	350	3800
Breakdown electric field ($MVcm^{-1}$)	0.3	0.4	3	5	10
Electron saturation velocity (cm/s)	1×10^7	2×10^7	2×10^7	2×10^7	3×10^7
Thermal conductivity ($W/cm.K$)	1.5	0.8	4.9	1.4	20
Relative permittivity	11.8	12.9	10	8.9	5.7

Table 1.1 shows the comparison of important physical properties of the well–known semiconductor materials including Si, $GaAs$, $4H-SiC$, GaN and diamond. Si and diamond are the only elemental wide bandgap materials known so far, while $GaAs$, $4H-SiC$ and GaN (and

other materials) are the compound semiconductor materials. Si is still the dominant semiconductor and its devices are still being developed such as ICs. The $GaAs$ (and InP) would still dominate in the field of optoelectronics and wireless applications. The development of Si and $GaAs$ electronics and their cost effectiveness, as compared with SiC, indicates that wide bandgap semiconductor devices are unlikely, in the future, to be used in low power electronics applications for temperatures up to 300°C. The $4H-SiC-$, $GaN-$ and diamond–based devices may be used for applications which are not satisfied by the existing Si or $GaAs$ technology. Although, diamond has superior physical properties for high–power and high–temperature electronics, the diamond–based electronics is not yet matured. Also several potential challenges are yet to be addressed in the device technology. On the other hand, GaN has a higher theoretical breakdown critical field compared to SiC, but the viable GaN substrate technology is not existed compared to that of SiC substrate. Due to which hetero–epitaxial growth of GaN on SiC and sapphire substrates are being frequently reported in the literature. This leading $GaN-$based devices to exhibit much lower breakdown voltages than expected. Thus, compared to GaN and diamond the $SiC-$based devices have the advantages of more matured technology of material growth as well as the device fabrication. This is one of the primary reasons for the commercialization of $SiC-$based SBDs, JFETs and MOSFETs in the recent years. Si and SiC have gained much importance not only due to their superior physical properties, but also due to their rich availability on Earth. This is a big advantage compared to noble metals and rare–earth elements [1].

Both Si and SiC crystals exhibit the covalent type of bonding. But, unlike Si, SiC does not exhibit complete covalent structure because of the difference in electronegativity between Si and C (with C being more electronegative than Si according to Pauling scale). This leading to $11-12\%$ of ionicity which gives to polarity property to SiC crystal [2]. The difference between Si and SiC is that Si crystallizes in diamond cubic form while SiC may crystallize in different forms depending on the stacking sequence of $Si-C$ bilayers (polytypism). More than 200 polytypes of SiC have been identified but the polytypes $3C-SiC$, $4H-SiC$, $6H-SiC$ and to some extent $15R-SiC$ have remained most popular [3, 4]. The stacking sequence of $3C-SiC$, $4H-SiC$ and $6H-SiC$ are $ABCABC$ ... $ABCBABCB$ ..., and $ABCACBABCACB$ ... respectively. The letter "C" in "$3C-SiC$" denotes the cubic crystal structure and "3" refers to the number of double–atomic layers in one repeating unit (ABC). "H" refers to the hexagonal crystal structure and the number before "H" denotes the number of double–atomic layers in one repeating unit. Among all the polytypes of SiC, $4H-SiC$ polytype exhibits superior properties [2]. However, the optimum performance of Si and $4H-SiC$ are limited by energy bandgap and their nature, unavoidable grown–in and process–induced defects as well as issues with metal contacts. At present, the quality of $4H-SiC$ wafers and metal contacts to its devices are the primary challenging issues than Si.

From the fundamental and technological point of view, it is important to examine the radiation effects on $4H-SiC$. One of the main consequences of the interaction of high energy radiations such as electrons, ions, neutrons, photons, or more exotic particles with materials is the formation of lattice defects. The lattice defects, whether simple or complicated are resulted from the energy transfer to the atoms [1, 3]. The overall radiation–induced modifications in the material are detrimental and sometimes useful for an application depending on the type, energy, flux and exposure time of the radiation. In the section 1.2, a general overview of the interaction of radiation with the matter has been presented. The fundamental radiation damage mechanisms in semiconductors and practical radiation environments have been also underlined in this section. From the practical point of view, the radiation effects on the electronic device properties are desirable. In this view, Schottky junctions (or Schottky contacts/Schottky diodes) have been explored in the present research. These devices are known to be sensitive to the modifications in the surface, interface and bulk electronic properties. Thus, a brief account on the formation of Schottky barrier in metal–semiconductor contact has been outlined in the section 1.3.

1.2. Interaction of neutrons with matter

Neutrons interact by both absorption and scattering processes. Unlike electrons or $\gamma-$rays, the interaction of neutrons with the electron cloud is weak but due to its neutral charge property the interaction with nuclei of the absorbing medium is very strong. As a result of which the neutron may either totally disappear and be replaced by one or more secondary radiations, or else the energy or direction of the neutron is changed significantly. The neutron interaction with the material medium varies dramatically depending on its energy. The slow neutron ($<$ $0.5\ eV$) interactions results in the elastic scattering with the absorber nuclei and a large set of different nuclear reactions can take place in the absorbing medium as shown in Fig. 1.1. The nuclear reactions modifies the atomic number and/or atomic mass number of the struck nucleus. If the energy of the fast neutron is sufficiently high ($0.5 - 20\ MeV$), inelastic scattering with nuclei can take place in which the recoil nucleus is elevated to one of its excited states during the collision. The nucleus quickly de–excites, emitting a $\gamma-$ray and the neutron loses a greater fraction of its energy than it would in an equivalent elastic collision. As the neutron energy decreases, scattering continues, but the probability of capture by a nucleus generally increases. If a neutron reaches thermal energies, it will move about randomly by elastic scattering until absorbed by a nucleus [4].

The capturing of thermal neutrons by atomic nucleus cause a new nucleus and the element remains unchanged or it decays, by transmuting into new element. This is known neutron transmutation doping (NTD). In silicon the phosphorous atoms are created in the beta decay of unstable ${}^{31}_{14}Si$ which forms when ${}^{30}_{14}Si$ captures the thermal neutrons i.e., ${}^{30}_{14}Si + n \rightarrow {}^{31}_{14}Si + \gamma \rightarrow {}^{31}_{15}P + \beta^{-}$. NTD depends on the abundance of the heavy isotope and its capturing cross section (Table 1.2). The extreme homogeneity and the excellent control of the phosphorus concentration in Si can be attained *via* NTD. However, the impurities present in the sample could affect the dopant concentration or may form complex defects in the material [5]. NTD in SiC is also reported by other researchers [6, 7].

The displacement lattice damage produces trap levels in the energy bandgap of the material. Such radiation–induced trap levels or defect states significantly influence the carrier mobility (μ), carrier density (n_c), resistivity (ρ) and generation and recombination lifetimes (τ) of a material [1, 8].

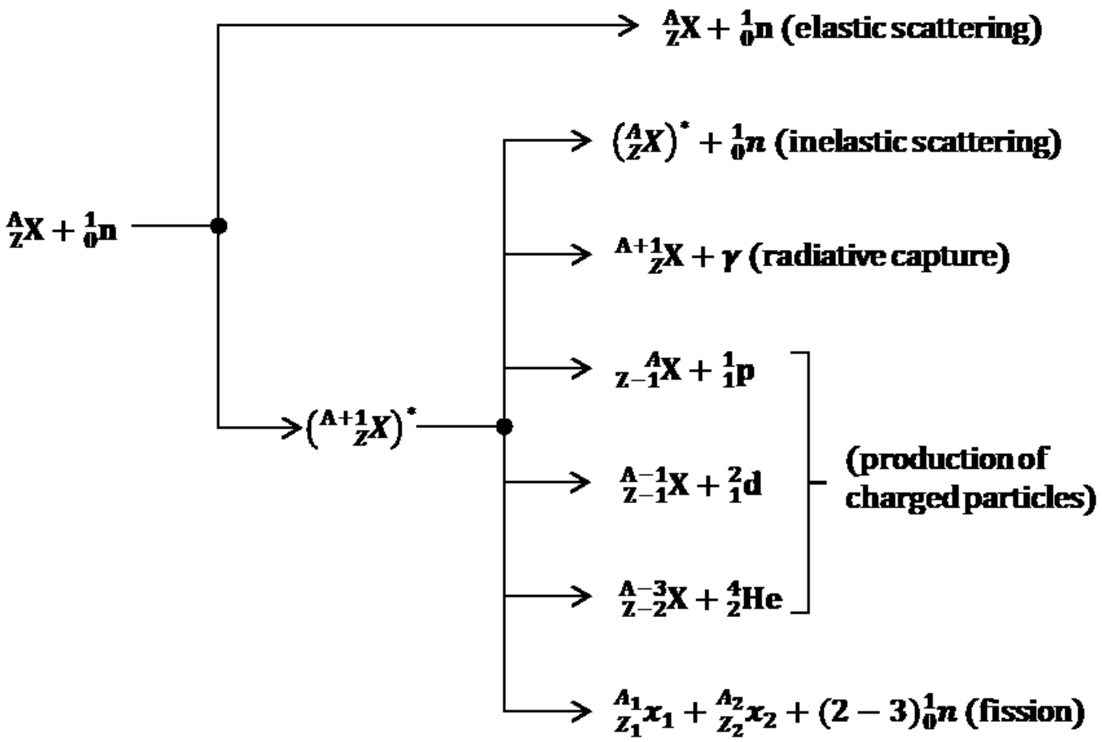

Fig. 1. 1. Different types of neutron–interaction and neutron–induced nuclear reactions.

Table 1.2. Different isotopes of C, O, N, Si, Al, and P and their neutron transmutation products.

Isotope	Abundance (%)	Thermal–neutron capture cross–section ($10^{-24} cm^2$)	Neutron transmutation product
${}^{12}_{6}C$	98.89	0.0034	${}^{13}_{6}C$
${}^{13}_{6}C$	1.11	9×10^{-4}	${}^{14}_{7}N$
${}^{14}_{7}N$	99.63	0.076	${}^{15}_{7}N$
${}^{15}_{7}N$	0.37	4×10^{-5}	${}^{16}_{8}O$
${}^{16}_{8}O$	99.76	1.78×10^{-4}	${}^{17}_{8}O$
${}^{17}_{8}O$	0.038	$0.235\ (n, \alpha)$	${}^{14}_{6}C + {}^{4}_{2}He \rightarrow {}^{14}_{7}N$
${}^{18}_{8}O$	0.204	1.58×10^{-4}	${}^{19}_{9}F$
${}^{28}_{14}Si$	92.23	0.17	${}^{29}_{14}Si$
${}^{29}_{14}Si$	4.67	0.10	${}^{30}_{14}Si$
${}^{30}_{14}Si$	3.10	0.11	${}^{31}_{15}P$
${}^{31}_{15}P$	100	0.18	${}^{32}_{16}S$

1.3. Schottky contacts

The Metal–Semiconductor ($M\!-\!S$) interface or contacts is an important aspect of microelectronics technology since every semiconductor device needs an interface to communicate with outside circuits. Basically two types of $M\!-\!S$ contacts exist in the microelectronics, the ohmic and rectifying contacts. In ohmic contacts the current flow occurs in both directions, while in the rectifying contacts the current flow occurs in only one direction (known as rectifying) as shown in Fig. 1.2.

The rectifying behaviour of $M-S$ contacts was first discovered by Ferdinand Braun in 1874. However, the physical understanding of rectification behaviour at $M-S$ contacts developed very slowly. A huge step forward was made by Walter H. Schottky and his collaborators. In 1938, Schottky reported the rectification of $M-S$ contacts by accounting band bending in the semiconductor at the interface. In order to honour Schottky's many contributions to the understanding of rectifying M–S contacts, they are generally labelled as Schottky contacts. Due to low noise level generated by Schottky contacts they are extensively used in the practical applications including the microwave receivers, detectors and mixers. Thus, the understanding of Schottky contact behaviour is crucial in the field of semiconductor device technology [1, 9, 10].

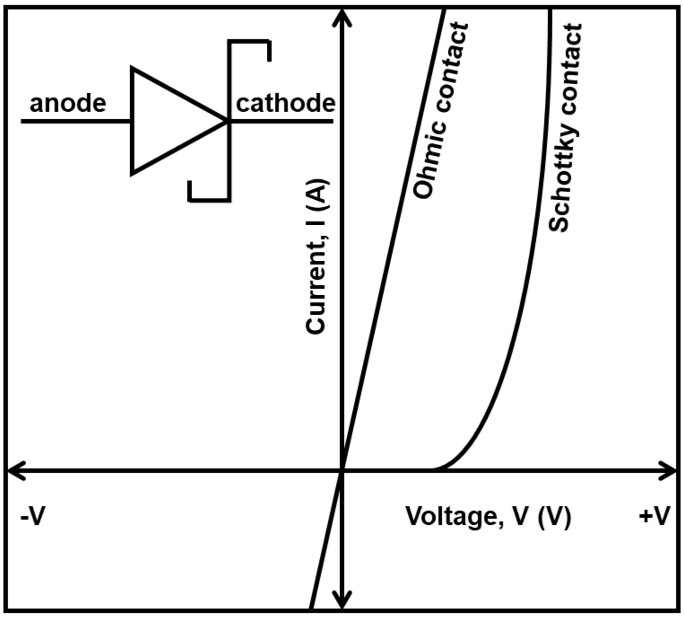

Fig. 1.2. $I-V$ characteristics of ohmic and Schottky contacts. Inset shows the circuit symbol for Schottky diode.

1.3.1. Formation of ideal Schottky barrier

Fig. 1.3 (a) shows the schematic representation of energy band diagrams for a metal and $n-$type semiconductor that are not in contact. In order to compare the relevant energy levels within and between two solids, we seek an energy level that is common to both solids and that is fixed with respect to both. That energy level is the vacuum level (E_0), which is defined as the energy that an electron is assumed to have if it were at rest outside and just free of the solid. The Fermi energy (E_F) represents the average energy of an electron in the system. For a metal, E_F is the average energy of the most energetic electrons. The energy difference between E_0 and E_F is labelled the work function (Φ) of the solid. Therefore Φ can be defined as the energy required to move an electron from E_F to E_0, where it is at rest and free of the influence of the solid. But in doped semiconductors, the position of E_F is not at a fixed level with respect to CB and VB as it depends on dopant concentration (N_D). In a given metal, however, E_F is located slightly above the bottom of the conduction band (E_C) and at a fixed separation from the vacuum level E_0. In a semiconductor, the bottom of the conduction band E_C is located at a fixed separation from E_0. The difference between E_0 and E_C in a semiconductor is known as electron affinity, denoted by χ_S. The electron affinity is therefore the energy which is needed to move an electron from the bottom of the E_C and to place it at rest outside the solid. From Fig. 3 (a) it has to be noted that if $\Phi_M > \Phi_S$, while the solids are separated, then the electrons in the metal have on the average a total energy that is lower than that of electrons in the semiconductor (and vice versa when $\Phi_M < \Phi_S$). Due to this reason, the Schottky diodes are also known as hot electron or hot carrier diode. Depending on the semiconductor type ($n-$ or $p-$) and work functions of the semiconductor and metal, one obtains either a Schottky or ohmic contact. Ideally, Schottky contact is ensued when $\Phi_M > \Phi_S$ (for $n-$type) and $\Phi_M < \Phi_S$ (for $p-$type), otherwise the contacts are ohmic in nature [1, 9, 10].

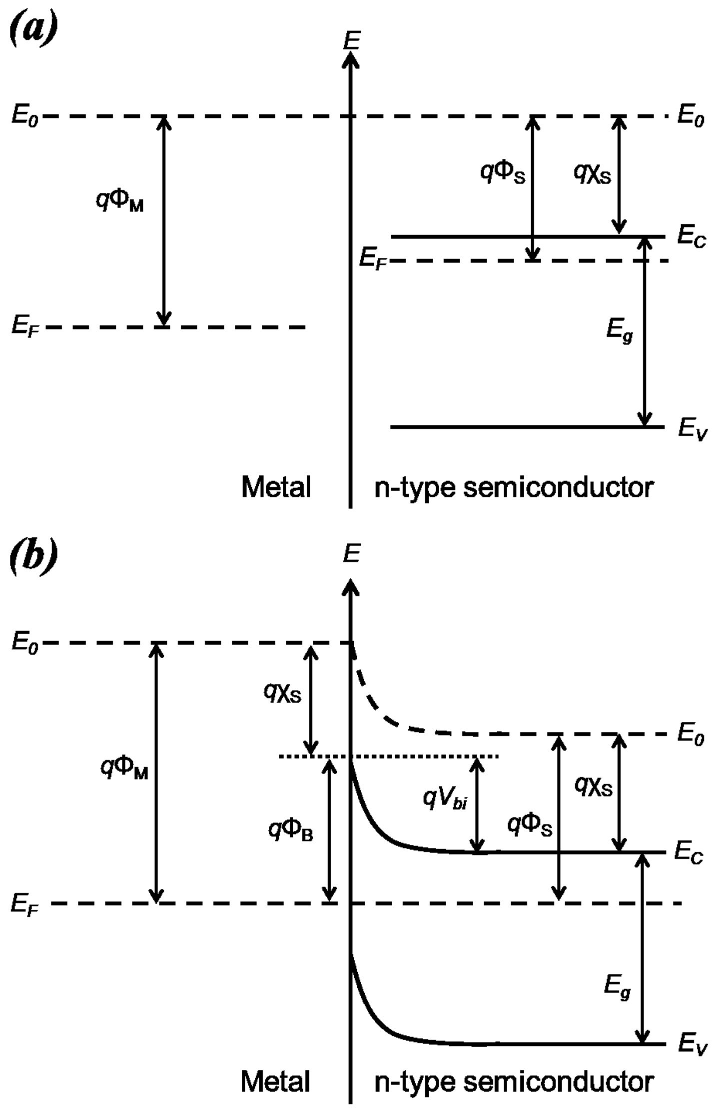

Fig. 1.3. Schematic representation of energy levels of metal and n−type semiconductor (a) not in contact; (b) conditions at equilibrium after contact formation.

Fig. 1.3 (*b*) shows the effects of the intimate contact on the energy levels and energy bands under equilibrium condition for $\Phi_M > \Phi_S$ (for n−type). At the instant of contact and since E_F of the semiconductor is higher than that of the metal, electrons will transfer from the semiconductor into metal until equilibrium is reached and E_F are aligned. As a result, at thermal equilibrium, the semiconductor is charged positively with respect to the metal. A depletion layer consisting of positively charged ionized donor atoms is established in the semiconductor.

This is coupled with a layer of excess electrons lining the surface of the metal in contact with the semiconductor. An electric field directed from the semiconductor to the metal is thus built and potential barrier (qV_{bi}) is established. This is accompanied by bending of the energy levels of the CB and of the VB in semiconductor in the region of the depletion layer. Since χ_S is assumed to be constant of the semiconductor, the bending of the CB is accompanied by an identical bending of the E_0 level. In both metal and semiconductor, the locus constant E_0 has not changed, it is still the energy that an electron has when it is free of the solid.

In contrast to the depletion layer (W_D), that is formed in the semiconductor, a surface sheet of electrons is formed in the metal. This is because the metal is assumed to be a perfect conductor with zero resistance, which does not permit the formation an electric field and sustaining of voltage drop. At thermal equilibrium, the distribution of density of electrons above E_C is identical in both the metal and the semiconductor. As a result, there will be continuous flow of electrons at the same rate in both directions with the result that the net current across the junction is zero. As can be seen from Fig. 1.3 (*b*) that there exist potential barrier which electrons must overcome on both sides of the junction. The barrier for the electrons that are in bulk of the semiconductor, which prevents them from moving into the metal and which they must overcome, is known as built–in potential (V_{bi}), which is given by

$$qV_{bi} = q(\Phi_m - \Phi_s) \tag{1.1}$$

On the other hand the barrier for electrons in the metal is known as Schottky barrier. The Schottky barrier height (Φ_B) represents the energy barrier that electrons in the metal must overcome to move into the semiconductor. It is the energy difference between aligned E_F and the semiconductor band edge at the surface with the metal. For an ideal contact $M-S$ Schottky contact Φ_B is given famous Schottky–Mott relationship [1, 9, 10]:

$$q\Phi_B = q(\Phi_M - \chi_s) \tag{1.2}$$

Thus for a given metal and semiconductor, Φ_B controls the junction properties. In the above discussion it is mentioned the term as ideal contact to indicate the calculated values for Φ_B according to Eq. (1.2), which means the linear dependence of Φ_B on Φ_M for a given semiconductor. But in reality, most practical contacts exhibit deviation from Eq. (1.3) due to Fermi–level–pinning (FLP) mechanism [9, 10]. Yet Eq. (1.2) is still be practically used to account for deviations from the theory and experiment.

1.3.2. Current–voltage characteristics of a Schottky contact

Biasing a Schottky contact is the process of connecting a voltage source between the metal and semiconductor. The biasing voltage depending upon its directions, causes the Schottky contact to conduct either in the forward direction or in the reverse direction. In the forward direction, a small voltage causes a large exponential increase in the current, whereas in the reverse direction the current increase is negligibly small unless the voltage is so high that breakdown occurs. The forward bias is achieved by connecting the positive lead of the voltage source to the metal contact and the negative lead to the n−type semiconductor contact. When the polarity is reversed then the Schottky contact is said to be operating in the reverse bias condition.

We now consider the conditions that ensue when the equilibrium (Fig 1.3 (b)) is disturbed by an applied voltage. Since V_{bi} at equilibrium appears only in the semiconductor and since metal cannot sustain any voltage drop, any voltage that is applied appears entirely on the semiconductor. Therefore, the barrier height Φ_B is unchanged and controls the transport mechanism across the junction. As a consequence, the density of electrons in the metal that have energies greater than this barrier is unchanged from the equilibrium value. An applied voltage causes a change in the bending of the bands in the semiconductor and a corresponding change in the electric field in the semiconductor at the junction with the metal. The barrier V_{bi}

in the semiconductor is reduced when a forward bias is applied which makes metal positive with respect to semiconductor. This reduces the electric field and the degree of bending of the bands. As the barrier reduced, more electrons, compared to thermal equilibrium, cross from the semiconductor to the metal. On the other hand, the number of electrons that cross from the metal to the semiconductor is unchanged from the number that crosses at equilibrium because the barrier height Φ_B, they have to surmount is unaffected by the applied voltage and unchanged from its thermal equilibrium value of Eq. (1.2). When the reverse–bias is applied to the junction, V_{bi} increases and limits the electron flow from semiconductor to metal while the barrier for electrons from metal to semiconductor (Φ_B) remains unchanged, it still has a same value according Eq. (1.2) of $q(\Phi_M - \chi_S)$ and therefore same current density as that of under equilibrium situation. Thus Φ_B controls the current–voltage ($I-V$) characteristics of a Schottky junction. Fig. 1.2 shows the $I-V$ characteristics of ideal Schottky contact.

According to thermionic–emission (TE) theory, the increase in the forward current (I) for the applied voltage (V) is given by the expression [9, 10]

$$I = I_S \left[\exp\left(\frac{qV}{kT}\right) - 1 \right] \tag{1.3}$$

where I_S is the reverse saturation current which is given by:

$$I_S = AA^{**}T^2 \exp\left(\frac{q\Phi_B}{kT}\right) \tag{1.4}$$

q is the charge of the electron, Φ_B is the Schottky barrier height, k is the Boltzmann constant, T is absolute temperature, A is the effective device area and A^{**} is the effective Richardson constant for thermionic–emission, which is given by,

$$A^{**} = 4\pi q m^* k^2 / h^3 \tag{1.5}$$

where $m^*$is the effective mass of the electron and h is the Planck constant.

However, most practical Schottky diodes exhibit deviations from the ideal Schottky diode Eq. (1.3). A parameter called the ideality factor (η) is introduced to account the non–ideal behaviour of the diode. The relation is given by

$$I = I_s \exp\left(\frac{qV}{\eta kT} - 1\right) \tag{1.6}$$

The parameters Φ_B and η can be determined from the Eq. (1.6).

Chapter 2

Literature Review

2.1. Radiation Effects on 4H-SiC Schottky Contacts

The radiation effects on Schottky contacts is questionable due to the interdependence of several processing parameters and/or techniques. For instance, the material growth, impurities, defects in the surface, bulk and interface before and after irradiation play crucial role in the understanding of junction properties.

Table 2.1. Radiation effects on different 4H-SiC Schottky contacts [N_D: dopant concentration; BI: Before Irradiation; AI: After Irradiation].

Schottky contact	**Methodology**	**N_D cm^{-3}**	**Radiation parameters**	**Schottky barrier height, eV**		**Ideality factor**	
				BI	**AI**	**BI**	**AI**
Ni/4H–SiC [11]	Thermal deposition	1×10^{14}	60 Co gamma; 1 MGy	2.12	1.92 (1 MGy)	1.87	1.88 (1 MGy)
Ni/4H-SiC [12]	Resistive evaporation technique; boiled in trichloroethylene ,acetone, methanol for 5 minutes each, then rinsed in deionized water and 40% conc. HF, then dried in nitrogen gas	3.4×10^{14}	electrons, strontium disc , 6.8×10^{9} cm-2 s-1	2.13	2.19 (5.4×10^{14} cm^{-2})	1.05	1.04 (5.4×10^{14} cm^{-2})
Al/n-4H-SiC [13]	Thermal evaporation; 40% HF for one minute and followed, by 1 min rinse in deionized water.	5×10^{16}	40 MeV Si ions; 1.5×10^{10} cm^{-2}	0.99	0.92 (1.5×10^{10} cm^{-2})	1.03	1.11 (1.5×10^{10} cm^{-2})
			25 MeV C ions; 1.7×10^{11} cm^{-2}	0.96	0.94(1.7×10^{10} cm-2)	1.02	1.09(1.7×10^{11} cm^{-2})
			1 MeV electrons; 2.0×10^{16} cm^{-2}	1.01	1.01(2×10^{10} cm^{-2})	1.01	1.03(2×10^{16} cm^{-2})

N_D: dopant concentration; BI: Before Irradiation; AI: After Irradiation

Schottky contact	Methodology	N_D cm^{-3}	Radiation parameters	Schottky barrier height, eV		Ideality factor	
				BI	AI	BI	AI
RuO_2/n-4H-SiC [14]	Magnetron sputter deposition	6.2×10^{15}	9 MeV electrons; 50 Gy	0.88	-	1.28	-
$RuWO_x$/n-4H-SiC [14]				0.70	0.51	1.16	1.433
Ni/4H-SiC [15]	Etched in 40% HF for 30 seconds, then rinsed in deionized water and followed by blowing dry with nitrogen gas prior to thermal evaporation of the nickel cleaned in an ultrasonic bath for three minutes each in trichloroethylene , acetone and methanol, followed by a 1 min rinse in deionized H2O	7.1×10^{15}	5.4 MeV alpha-particles	1.25	1.31	1.04	1.07
Ni/4H-SiC [16]	Thermal Evaporation; Samples were also cleaned in ultrasonic water bath for three minutes each in trichloroethylene ,acetone and methanol followed by one minute rinsed in deionized water after the annealing of the ohmic contact	1.9×10^{16}	Alpha-particle fluence of (9.2×10^{11} cm^{-2})	1.47	1.34	1.2	1.85
Ni/n-4H-SiC [17]	Deposition; Ni and TI are sputtered on silicon and carbon side respectively to form a Bi layer contact	5×10^{14}	60 Co gamma; 110 Mrad	1.2	0.88eV (110 Mrad)	1.33	24 (110 Mrad)

N_D: dopant concentration; BI: Before Irradiation; AI: After Irradiation

Table 2.1 gives a broad overview of radiation effects in SiC based Schottky barrier diodes. One can clearly see that the Schottky diode parameters such as Schottky barrier height and ideality factor are strongly dependent on the type of metal, dopant concentration, type of radiation and exposure time (fluence) and processing techniques. It is also evident that there is no clear correlation between the variation in the barrier height and dopant concentration. However, majority of the studies have shown decrease in the Schottky barrier height and an increase in ideality factor. These modifications are the consequences of influence of radiation induced defects in the surface, interface and bulk of the material [1]

2.2. Research Objectives

One of the research gaps found from the literature review is that the despite there exist many reports on radiation effects on 4H-SiC based Schottky contacts, still there is a need for reports for different radiation environments and for different type of 4H-SiC based Schottky contacts. In addition, the structural and optical property changes are also needed to understand the radiation effects. In this view, the objectives of the present research study are as follows:

i. To examine the structural and optical properties of thermal neutron irradiated n-type 4H-SiC.
ii. To prepare and study the thermal neutron irradiation effects on Al/n-4H-SiC Schottky contacts.

Chapter 3

Experimental Techniques and Methodology

In this chapter the basic principles of different characterization techniques used in the present research are outlined. The chapter includes details of the materials used, preparation of Schottky contacts, radiations used for irradiating the samples. In addition the details of different techniques used such as X–ray Diffraction (XRD), Raman spectroscopy (RS), UV–Visible optical absorption spectroscopy, photoluminescence Spectroscopy (PLS), and current–voltage ($I-V$) characterisation are detailed.

3.1. Materials

The commercially on the market customary two inch n-type 4H-SiC < 0001 > wafers were procured from Semiconductor Wafer, Inc. Taiwan. The wafer was polished on each of the edges and doped with nitrogen. The resistivity of the sample was 0.012−0.03Ω.cm (5×10^{18} cm^{-3}) and the micropipe density was ≤ 30 cm^{-2}. The density and thickness of the wafer was 3.21 and 330±25 μm respectively.

3.2. Schottky Contact Fabrication

The procured n–4H–SiC wafers were diced into 1×1 cm squares using a diamond tip scriber. These diced samples were then cleansed in line with the standard procedures. The method consisted of following consecutive steps. Primarily, degreasing samples in acetone/methanol (99.9%), followed by rinse with running deionized (DI) water for five minutes. After that, the samples were dipped into 2% diluted hydrofluoric (HF) for two minutes to etch the native oxide layer on n–4H–SiC, and again rinsing in running DI water for five minutes. The cleansed samples were then loaded into the chamber for thermal deposition of Al Schottky metal contacts. The Al wire (99.9%) was placed in the tungsten boat in a very high vacuum that is then heated to its evaporation purpose by heating the Tungsten boat. During this process, the gaseous molecules of Al travel from supply to the n–4H–SiC substrate wherever they nucleate together and form a thin coating of Al. A ready shadow mask of circular diameters 0.2 and 0.4 were used to get the Schottky contacts. The deposition was applied at the speed of 3Å/s in the vacuum of 8×10^{-6} mbar. The thickness of Al was unbroken within the range of ~50 nm by monitoring through a digital thickness monitor (DTM).

3.3. Neutron Radiation Source

The neutron irradiation (NI) on the diced samples and as–prepared Schottky contacts were carried out at Dhruva research nuclear reactor, Bhabha Atomic Research Centre (BARC) Trombay India. The samples were packed in the Al foil and kept for irradiation in the reactor environment at room temperature. The approximate energies of neutrons were of the order of $100\, meV$ (thermal neutrons) and the average flux at the sample position was $\sim 1.5 \times 10^{13}\, ncm^{-2}s^{-1}$. All the samples were irradiated up to the fluence of ~$7.5 \times 10^{16}\, ncm^{-2}$ $(1.4\, h)$. After NI, the samples were kept under a cooling period of $\sim 24h$ [1, 18].

3.4. Characterization Techniques

3.4.1. X–ray diffraction (XRD)

XRD is widely used in the structural characterization of semiconductors. It is a non–destructive method with penetration from the surfaces into the bulk of the materials. The basic principle behind XRD is the scattering of $X-$rays from atoms of the crystal. If the scattered waves are in phase (coherent), they interfere in a constructive way and gives diffracted beams in specific directions (known as reflections). These directions are governed by the wavelength of the incident radiation and nature of the crystalline sample. The relation connecting wavelength of the X–rays to the spacing of the atomic planes is given by

$$n\lambda = 2d_{hkl}\, sin\, \theta \tag{3.1}$$

where n is an integer number, λ is wavelength of $X-$rays used, d_{hkl} is the interplanar separation of the crystal planes of the sample having Miller indices (hkl). The angle between the plane of the sample and the $X-$ray source is θ, the Bragg angle. The angle between the projection of the $X-$ray source and the detector is 2θ. For this reason the XRD patterns produced with this geometry are often known as $\theta - 2\theta$ scans. In this geometry the $X-$ray source is fixed, and the detector moves through a range of angles. The radius of the focusing circle is not constant but increases as the angle 2θ decreases [1].

The $X-$rays are generated by directing an electron beam of high voltage at a metal target anode inside an evacuated $X-$ray tube. Copper is the most frequently used target, and typical operating conditions are $40\ kV$ and $10 - 30\ mA$. In most diffractometers, a fixed value of the $X-$ray wavelength λ is used. $Cu\ K\alpha$ is widely used as a source of $X-$rays because of its high intensity. The weighted average wavelength of $Cu\ K\alpha$ is 1.54184 Å. An image produced by diffractometer is called Diffractogram. The XRD studies on $n-Si$ and $n-4H-SiC$ were carried out before and after irradiation. The XRD patterns were collected in 2θ range of 20– 80° using bench top Bruker D2 Phaser ($\lambda = 1.54184$ Å$, 30\ kV, 10\ mA$) under $\theta-2\theta$ geometry condition. From the obtained XRD patterns, the lattice parameters were estimated using the relevant expressions [18].

3.4.2. Raman spectroscopy (RS)

RS in solids deals with the inelastic scattering of light by phonons (or lattice vibrations). The phonons are very sensitive to the local structure and lattice environment. The relation between the incident and the scattered light is governed by the corresponding Raman scattering selection rules, which are determined by the lattice symmetry and the nature of the crystal. In most cases the Stokes–shifted lines i.e., scattered light that has an energy that is lower than that of the incident light by an amount equal to the energies of the emitted phonons are monitored in RS. These phonon modes are characterized by their intensity, energy, wave vector and polarization. Thus making a highly sensitive to the material under study [1].

The basic principle is that a sample is normally illuminated with a laser beam, then the scattered light is collected with a lens and is sent through interference filter or spectrophotometer to obtain Raman spectrum of a sample. In the present study, the Raman spectra of $n-4H-SiC$ were recorded in the back scattering symmetry using Jobin Yvon Horiba LABRAM–HR visible spectrometer. The Raman spectra is measured by exciting sample with $473\ nm$ line of an Ar^{+} laser which was focused on $1 \times 1\ \mu m^{2}$ spot. The Raman frequency is calibrated by known emission line of silicon ($520.6\ cm^{-1}$). The uncertainties in the Raman frequencies were estimated to be less than $1\ cm^{-1}$ [18]

3.4.3. UV–Visible absorption spectroscopy

When light from the source penetrates the semiconductor material it undergoes several absorption events in the material. The important absorption process is the fundamental absorption i.e., transition of electrons from VB to the CB. This provide fundamental knowledge about optical energy bandgap (E_g) of the semiconductor material. The absorption spectra can also show defect related signatures of the material [1, 2].

The optical absorption spectra of a semiconductor material can be obtained by using a spectrophotometer. This instrument is a combination of several spectroscopic components which includes light source, monochromator or filter, cuvette compartment, detector and amplifier with an indicating device. The commercially available UV–1800 UV–Visible Spectrophotometer was used to measure the absorption spectrum of $n-4H-SiC$. The spectra was measured for the photon propagation along c–axis direction of the crystal i.e., the electric field vector ($\vec{E}$) of the photons was perpendicular to c–axis of the crystal ($\vec{E} \perp \hat{c}$). From the obtained spectra E_g and E_U (Urbach energy) studies were carried out before and after irradiation. The optical absorption coefficient (α) after irradiation was calculated by assuming uniformity in the damage over the whole thickness, which allows a direct calculation based on Beer–Lambert law and in all cases the refractive index was assumed to be unchanged.

3.4.4. Photoluminescence spectroscopy (PLS)

PLS is a widely used qualitative technique for assessing the defect states and purity of semiconductor materials. When the optical absorption process generates excess number of carriers ($e-h$ pairs), they come back to the equilibrium by carrier recombination process. In the process of recombination, excess electrons of the CB fall down spontaneously to the VB and then recombine with excess holes. The energy released during recombination process is emitted as a photon. This emission is known as PL. The transitions other than band to band can also occur when there exists defects and impurities in the otherwise forbidden bandgap. Therefore the energy of the emitted photon are the characteristic of a defect level or donor levels [1].

In the present study PLS was used in particular to study the defect related luminescence features in $n-4H-SiC$ before and after irradiation. The PL spectra were measured using commercially available Horiba Jobin Yvon 450 W Illuminator. This spectrofluorometer features $450\,W$ ozone free Xe source and power supply double Czerny Turner emission spectrometer with $1200 g/mm$ grating blazed at $500\ nm$. The spectra was measured at room temperature in the wavelength range of $350-620\ nm$ at an excitation wavelength of $325\ nm$. The PL spectra was collected in the back–scattered geometry [18].

3.4.5. Current–voltage ($I-V$) Characterisation

The basic principle of measuring $I-V$ characteristics a Schottky junction is that applying the voltage (V) between two terminals and measuring the current (I) flowing across it. Under forward biasing condition, the positive terminal of the voltage source is connected to the Schottky metal contact and the negative terminal of the voltage source is connected to the ohmic contact. In the present study the $I-V$ characteristics of $Al/n-4H-SiC$ Schottky junctions were carried out using Keithley 2450 source meter. The spring loaded pressure contacts were used as back ohmic contacts during characterisation [1, 18].

Chapter 4

Results and discussion

In this chapter the effect of thermal neutron irradiation (NI) on the structural, optical and Schottky junction properties of $n-4H-SiC$ are detailed. The structural studies were carried out by estimating the change in the crystal lattice parameter and phonon modes before and after NI. In addition, the optical absorption and PL studies are carried out for $n-4H-SiC$. Finally, the NI effects on the Schottky properties were accounted by analysing $I-V$ characteristics of $Al/n-4H-SiC$ Schottky contacts.

Generally, the thermal neutron irradiation on silicon carbide basically forms different isotopes in the material. Both silicon and carbon have different stable isotopes. The natural silicon is a mixture of three different isotopes, namely, ${}^{28}_{14}Si$, ${}^{29}_{14}Si$ and ${}^{30}_{14}Si$ with abundance of 92.23, 4.67 and 3.10% respectively. Depending on the thermal neutron capture cross–section ${}^{28}_{14}Si$, ${}^{29}_{14}Si$ and ${}^{30}_{14}Si$ transmute into ${}^{29}_{14}Si$, ${}^{30}_{14}Si$ and ${}^{31}_{15}P$ respectively. While, carbon has two isotopes namely, ${}^{12}_{6}C$ and ${}^{13}_{6}C$ with abundance of 98.89 and 1.11% respectively. Depending on the thermal neutron capture cross–section ${}^{12}_{6}C$ and ${}^{13}_{6}C$ transmute into ${}^{13}_{6}C$ and ${}^{14}_{7}N$. But nitrogen transmutation is very inefficient as the capturing cross section is very low [Chapter 1, Table 1.2,]. However, reactor flux of thermal neutrons is always accompanied with fast neutrons ($E > 0.1\ MeV$), which may also cause displacement effects and generates defects such as vacancies or defect complexes in the material [5-8, 19].

4. 1. XRD analysis

The $4H-SiC$ $< 0001 >$ crystallizes in the hexagonal form having $P6_3mc$ (C^4_{6v}) space group. Accordingly, the XRD pattern mainly involves $(000l)$ reflections, where $l = 2n$ and n is an integer [20, 21]. For the unirradiated sample the (0008) peaks which corresponds to $n = 4$ was noticed at $2\theta = 75.62°$. As noticed, irradiated sample have shown peak shift towards the higher side after NI at the irradiation fluence of $\sim 7.5 \times 10^{16}\, n\, cm^{-2}$. This suggesting a decrease in the c −axis lattice constant of the material, where c can be evaluated by using the relation

$$c = \frac{\lambda \cdot l}{2 \sin \theta_{00l}} \tag{4.1}$$

By using above Eq. (4.1) the c −axis lattice parameter was estimated and its change ($\Delta c/c$) was found to be 2.8×10^{-3}. Such a decrease in c −axis lattice parameter is attributed to neutron –induced isotopic modifications in the material. The similar decrease in lattice parameter has been noticed in diamond with the increase of ${}^{13}_{6}C$ isotope [5, 22].

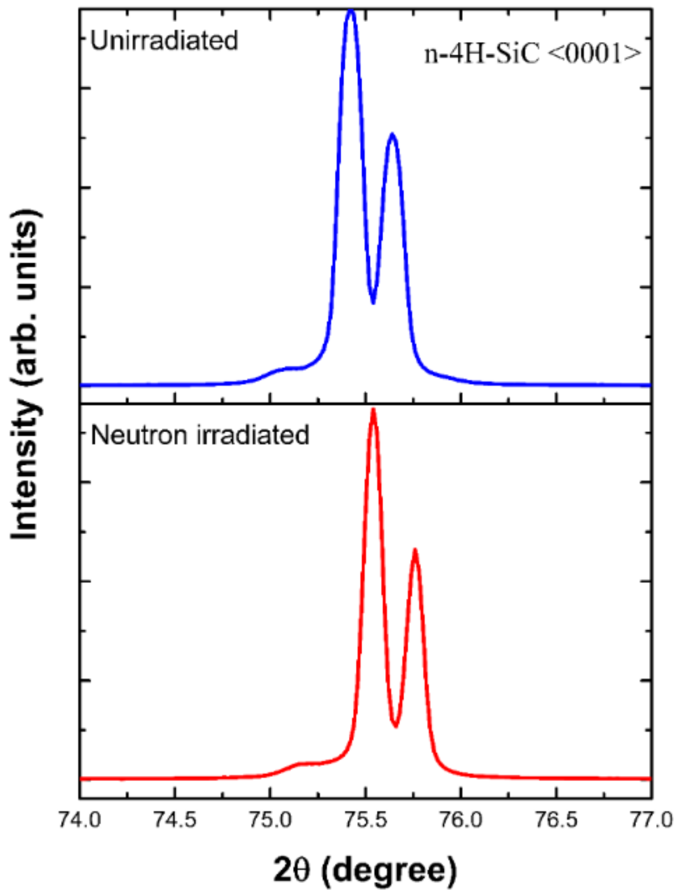

Fig. 4.1. XRD depicting (0008) XRD reflection of $n\!-4H\!-SiC$ before and after neutron irradiation.

4.2. UV–Vis absorption spectra analysis

Fig. 6.2 shows the optical absorption spectra of $n\text{–}4H\text{–}SiC$ before and after NI at the irradiation fluence of $\sim 7.5 \times 10^{16}\ ncm^{-2}$. The four characteristic features as marked are the representative of band to band (a), band to donor level and extended states (Urbach tail) (b), free electron absorption into higher conduction bands (c) and bands from defect states (d). The doping type, n-type (or p-type) can be seen from the presence (or absence) of the free electron absorption band or Biedermann absorption bands (c). These bands are known to be responsible for the green-brownish colour of polytypes [2].

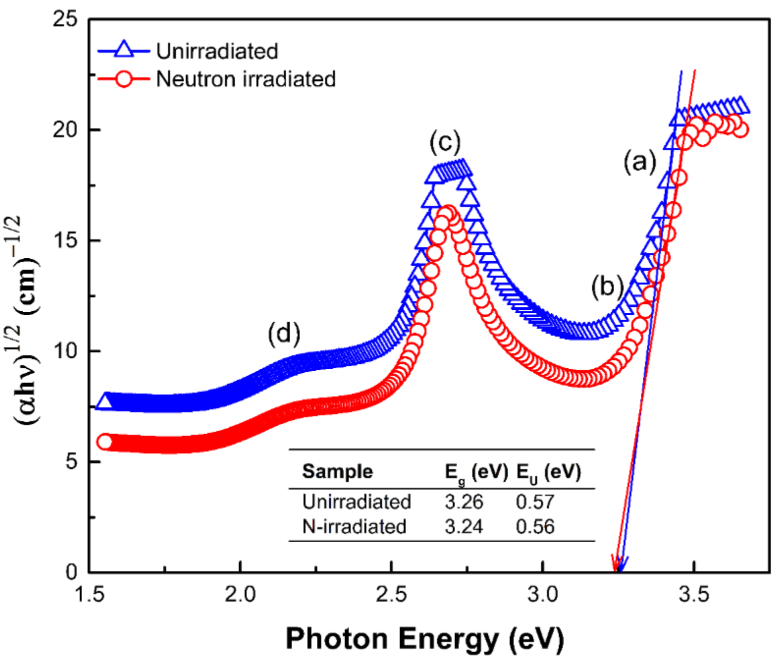

Fig. 4.2. Absorption spectra of $n\text{–}4H\text{–}SiC$ before and after neutron irradiation (inset table shows the variation in optical energy bandgap (E_g) and Urbach energy (E_U)).

After NI, marginal variations in the absorption spectra were observed such as shift in the absorption band edge (a), increased tailing (or widening) of the absorption edge (b) and the narrowing of absorption bands (c) and (d). By fitting Tauc's equation [23] for an indirect allowed transitions in the region (a), the band gap E_g of the sample was estimated. A decrease of $\sim 0.2\ eV$ in E_g has been noticed in the material. While well below E_g, the estimation of Urbach energy E_U ($\alpha \approx \exp\left(\frac{h\nu}{E_U}\right)$) has resulted in decrease of $\sim 0.01\ eV$. Thus as seen from Fig. 4.2 the overall decrease in absorption coefficient α, E_g and E_U of the irradiated sample could be caused due to isotopic modifications induced by thermal neutrons in the material.

4.3. Raman spectra analysis

Fig. 4.3 shows the first order Raman spectra (FORS) of $n-4H-SiC$ before and after NI. The different phonon modes are labelled in the spectra [1]. The neutron irradiated sample showed a downward shift in the LOPC mode about 5.7 cm^{-1} (Fig. 4.3, inset). But no significant modifications were noticed in the E_2(FTO) mode. A similar downward shift in the LOPC mode has been reported previously in the neutron irradiated $n-4H-SiC$ [24]. Such a shift towards lower phonon frequencies indicates a decrease in the free carrier concentration n_e of $n-4H-SiC$.

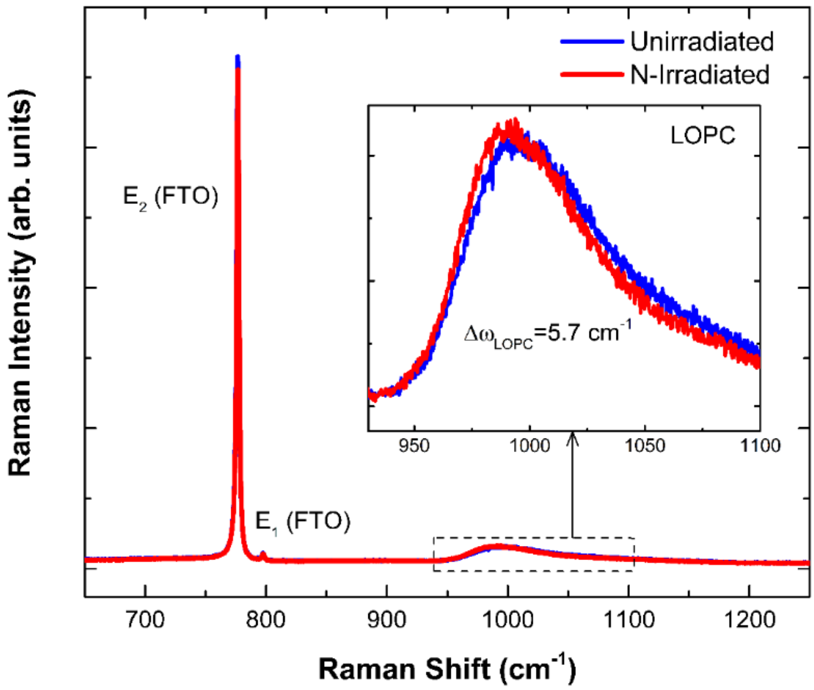

Fig. 4.3. First order Raman spectra of $n-4H-SiC$ before and after neutron irradiation. The inset plot shows the modification in the LOPC mode.

By considering an empirical relation,

$n_e = \Delta\omega^{1.0} \times 1.23 \times 10^{17}\ \mathrm{cm}^{-3}$

deduced by Nakashima *et al.* [25], it is estimated that n_e of the unirradiated and neutron irradiated samples were found to be 4.2×10^{18} and $3.5 \times 10^{18} cm^{-3}$ respectively. Such a decrease in n_e of the neutron–irradiated sample suggests the capture of free charge carriers by native defects or complex irradiation–induced defects in the material (compensation effects).

4.4. PL spectra analysis

Fig. 4.4 shows the PL spectra of $n-4H-SiC$ before and after NI measured at $\sim 300\ K$ and $325\ nm$ excitation. As noticed the distribution of PL intensity is remarkably varied after NI. A broad defect related PL band (DPL) around $\sim 2.35\ eV$ is observed in both the samples. The main radiative recombination path of DPL occurs *via* donor–acceptor pairs (DAP) of the $N-$ impurities and $N-$impurities associated with the intrinsic defects such as V_C and C_i (carbon interstitials) [26]. On the other hand a broad but less intense PL band observed near the band edge is attributed to recombination of nitrogen bound excitons (NBE) [27, 28]. But, NBE PL signal has not been observed in the neutron–irradiated sample. The similar quenching effects have been reported in the high energy NI on 4H–SiC, where the authors attribute such effects for lattice damage [27]. The PL quenching could be caused due to the passivation of dopants ($N-$ or NI–induced $P-$ dopants) by defect complexes, which may in turn leading to charge carrier compensation effects or decrease in n_e. The decrease in n_e is also evident from LOPC modes (Fig. 4.3). This leading to the increase in the DPL signal as opposed to that of the NBE band. Unlike the appearance NBE in $n-4H-SiC$, no clear PL signals of $P-$ dopants detected at room temperature.

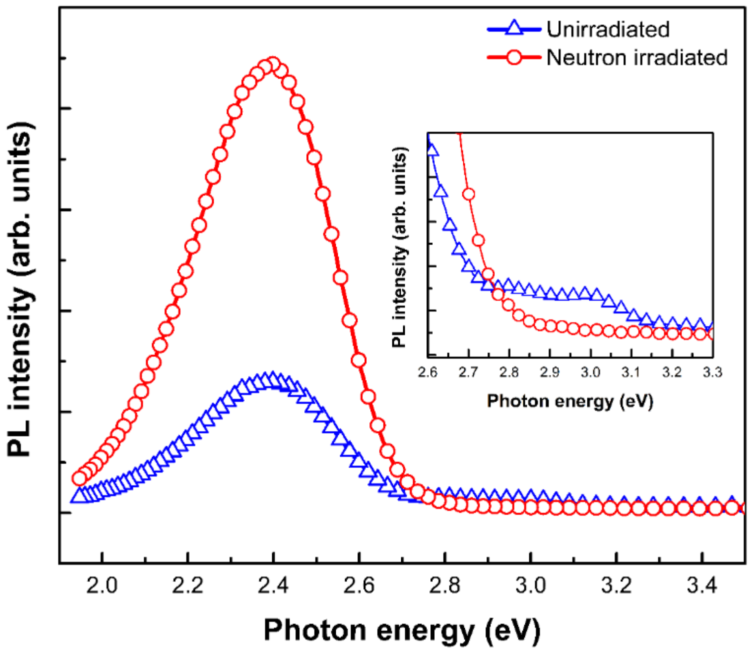

Fig. 4.4. Room temperature photoluminescence (RTPL) spectra of $n-4H-SiC$ before and after neutron irradiation.

4.5. Electrical studies on $Al/n-4H-SiC$ Schottky contacts

Fig. 4.5 shows the $I-V$ characteristics of $Al/n-4H-SiC$ Schottky junctions before and after NI at the fluence of ~$7.5 \times 10^{16}\ ncm^{-2}$. The decrease in the forward and reverse currents could be caused due to compensation effects in $n-4H-SiC$. The Schottky contact parameters η and Φ_B were evaluated applying thermionic emission model as follows:

According to thermionic emission (TE) theory, the expression for forward current (I) through the Schottky barrier (Φ_B) when the applied voltage (V) is given by [9, 10]

$$I = I_s\left[\exp\left(\frac{qV}{\eta kT}\right) - 1\right] \tag{4.2}$$

where, $$I_s = AA^{**}T^2 \exp\left(-\frac{q\Phi_B}{kT}\right) \tag{4.3}$$

is the reverse saturation current, A is effective area of the diode, A^{**} is the Richardson constant (for $n-4H-SiC$, $A^{**} = 146\ A \cdot cm^{-2}K^{-2}$ [2]), q is charge of the electron, Φ_B is Schottky barrier height, k is Boltzmann constant and T is absolute temperature. The parameter η in Eq. (4.5) is known as ideality factor, which accounts for non–ideal behaviour of a Schottky contact [1, 9, 10].

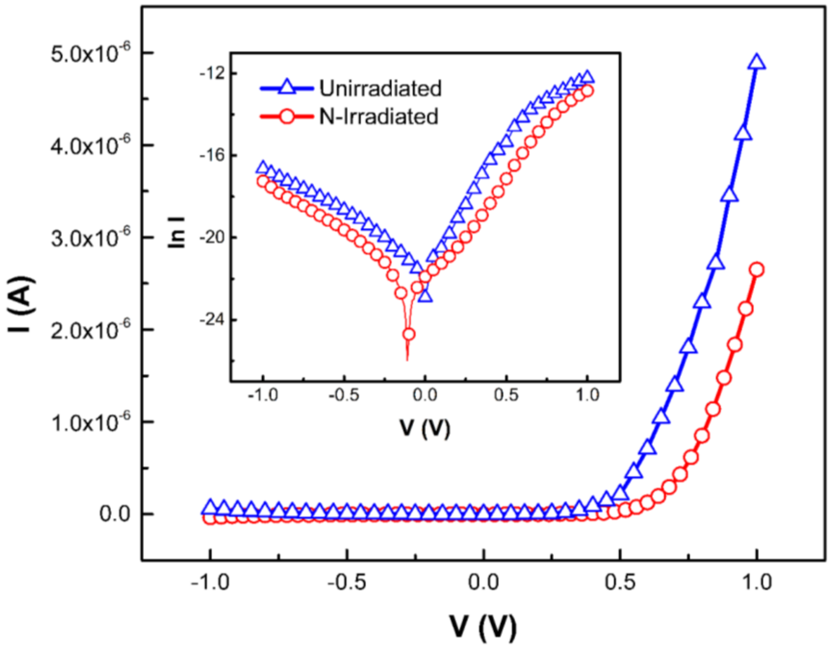

Fig. 4.5. $I-V$ characteristics of $Al/n-4H-SiC$ Schottky contacts before and after neutron irradiation. Inset shows the semi–log plot of the $I-V$ characteristics.

For $V > 3kT/q$, the term $-I_s$ in Eq. (4.5) can be neglected. One obtains a linear polynomial equation of the form:

$$\ln \mathrm{I} = \frac{qV}{\eta kT} + \ln I_S \tag{4.4}$$

Thus by plotting $\ln I$ vs. V one can obtain Φ_B and η from the intercept and slope respectively. These parameters can be evaluated by using the following expressions:

$$\eta = \frac{\mathrm{q}}{\mathrm{kT}} \frac{dV}{d(\ln I)} \tag{4.5}$$

$$\Phi_B = \frac{kT}{q} \ln\left(\frac{AA^{**}T^2}{I_s}\right) \tag{4.6}$$

The semi log plots are shown Fig. 4.6 respectively. The obtained values from these plots are reported in Table 4.1.

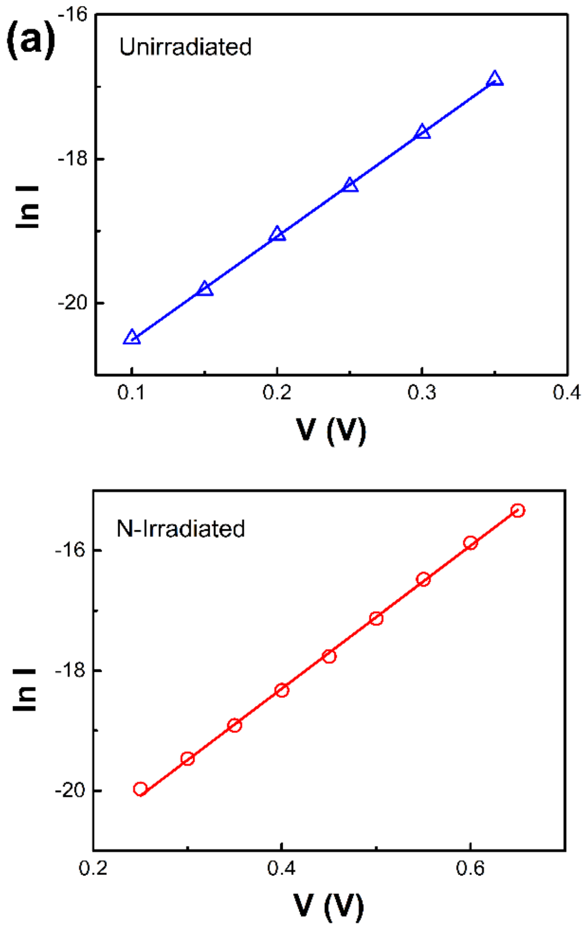

Fig. 4.6. Semi–log plots of $Al/n\!-4H\!-SiC$ Schottky contacts before and after neutron irradiation.

Table 4.1: The $Al/n\!-4H\!-SiC$ Schottky contact parameters before and after neutron irradiation.

Sample	TE Model	
	η	Φ_B (eV)
Unirradiated	2.69	0.90
N–Irradiated	3.25	0.93

Both the Schottky contacts showed $\eta > 1$, indicating the inhomogeneous or non–ideal nature of the Schottky junction [9, 10]. The obtained Φ_B value of 0.91 eV showed the pinning of E_F due to the presence of defect level at $E_c - 2.35\ eV$ as was detailed in section 4.4. On the other hand the increase in η and Φ_B of neutron irradiated $Al/n\!-4H\!-SiC$ Schottky junction is mainly attributed to neutron–induced modifications in $n\!-4H\!-SiC$ i.e., decrease in lattice parameter due to isotopic effects (Fig. 4.1) and decrease in n_e (inset, Fig. 4.2) due to formation of defects in $n\!-4H\!-SiC$ (Fig. 4.4). The zero–bias offset in the neutron–irradiated Schottky contacts is also attributed to the influence of defect states and their assistance in the tunneling mechanism across the Schottky barrier. Overall, noticeable modifications in the structural, optical and electrical properties were observed in the neutron irradiated samples.

To sum up, the thermal neutron irradiation showed decrease in the c −axis lattice parameter, E_g, E_U, n_e and H_V due to isotopic modification in $n\!-4H\!-SiC$. The decrease in n_e is attributed to compensation effects i.e., the capture of the free carriers by point defects such as carbon–related defect states. This has led to increase in the Schottky junction parameters of $Al/n\!-4H\!-SiC$ as well as zero–bias offset in the $I\!-V$ characteristics.

Chapter 5

Conclusion and Future Work

5.1. Conclusion

The thermal neutron irradiation effects on the structural, optical and electrical properties of n-4H–SiC and n-Al/n-4H–SiC Schottky contacts were studied. XRD studies revealed a decrease in the lattice parameter of the irradiated samples due to isotopic modifications and irradiation-induced defects in the material. The energy bandgap (E_g), Urbach energy (E_U), free carrier concentration (n_e) and PL bands of n-4H–SiC were noticeably affected due to isotopic modification and accumulation of defects in the material. Due to which the I–V characteristics of Al/n-4H–SiC Schottky contacts were substantially affected in terms of irradiation induced zero-bias offset as well as increase in the contact parameters such as Φ_B and η of the junction.

5.2. Future Work

In the present thesis, the structural, optical properties of n-4H-SiC and electrical properties of Al/n-4H-SiC Schottky contacts studied before and after thermal neutron irradiation. The studies are limited to thermal neutrons only and to only Al/n-4H-SiC Schottky contacts. One can extend the studies for different types of radiations at different radiation parameters such as radiation energy, radiation flux and radiation dose delivered. The studies can also be extended for different Schottky contacts as well.

Examining the irradiated sample by means of high–resolution SEM or TEM techniques would be helpful in probing the structural modifications

The room temperature I-V characteristics give limited information of the junction properties. Therefore it would be interesting to extend the studies by carrying out temperature dependent I-V characterisation over a wide temperature range. These studies gives more insight into the junction properties as well different transport mechanisms, particularly tunneling mechanism which is prevalent in wide band gap semiconductors.

There is still a need of defect characterisation by using different techniques such as EPR, DLTS, LTPL etc. Such studies would contribute substantially in the prospects SiC–based electronics.

References

[1] I. P. Vali, *Effect of radiation on structural mechanical and electrical properties of silicon based materials*, PhD thesis (2020) Manipal Academy of Higher Education, Manipal, India.

[2] T. Kimoto, J. A. Cooper, *Fundamentals of Silicon Carbide Technology: Growth, Characterization, Devices and Applications*, Wiley (2014).

[3] K. Nordlund, S. J. Zinkle, A. E. Sand, F. Granberg, R. S. Averback, R. E. Stoller, T. Suzudo, L. Malerba, F. Banhart, W. J. Weber, F. Willaime, S. L. Dudarev, D. Simeone, *Primary radiation damage: A review of current understanding and models*, J. Nucl. Mater. 512 (2018) 450–479.

[4] G. F. Knoll, *Radiation detection and measurement*, Wiley (1988).

[5] E. E. Haller, *Isotopically engineered semiconductors*, J. Appl. Phys. 77, 2857 (1995).

[6] S. Tamura, T. Kimoto, H. Matsunami, M. Okada, S. Kanazawa and I. Kimura, *Nuclear transmutation doping of phosphorous into 6H–SiC*, Materials Science Forum 338–342 (2000) 849–852.

[7] H. Heissenstein, H. Sadowski, R. Helbig, *Defect correlated emmission and electrical properties of 4H–and 6H–SiC epitaxial layers doped by nuclear transmutation doping (NTD)*, Physica B 308–310 (2001) 702–705

[8] C. Claeys, E. Simoen, *Radiation Effects in Advanced Semiconductor Materials and Devices*, Springer (2002).

[9] S.M. Sze, *Physics of Semiconductor Devices*, Second Edition, Wiley (1981).

[10] E. H. Rhoderick and R. H. Williams, *Metal–Semiconductor Contacts*, Second Edition, Oxford Science Publication (1988).

[11] Zheng Li, Jian Wu, Kunlin Wu , Yikui Fan, Zhongxiong Bai, Yong Jiang ,Yanpeng Yin, Qilin Xie , Jiarong Lei. *The performance of 4H–SiC detector at high temperature after gamma Irradiation,* Radiation Physics and Chemistry 162 (2019) 153–156.

[12] A.T. Paradzah, E. Omotoso, M.J. Legodi, F.D. Auret, W. E. Meyer, and m. diale *Electrical Characterization of High Energy Electron Irradiated Ni/4H-SiC Schottky Barrier Diodes,* Journal of Electronic Materials 45 (2016) 4177-4182.

[13] Heyi Li, Chaoming Liu, Yanqing Zhang, Chunhua Qi, Yidan Wei, Jiaming Zhou, Tianqi Wang, Guoliang Ma, Zujun Wang, Shangli Dong and Mingxue Huo, *Irradiation effect of primary knock-on atoms on conductivity compensation in N-type 4H-SiC Schottky diode under various irradiations.* Semiconductor Science and Technology 34 (2019).

[14] Stuchlikova, Lubica & Harmatha, Ladislav & Buc, Dalibor & Benkovska, Jana & Hlinka, B. & Siu, G.. *4H-SiC Diode with a RuOx and a RuWOx Schottky Contact Irradiated by Fast Electrons*. Conference Proceedings - The 6th International Conference on Advanced Semiconductor Devices and Microsystems (2006). ASDAM'06. 10.1109/ASDAM.2006.331187.

[15] E. Omotoso , W.E. Meyer, F.D. Auret, A.T. Paradzah, M. Diale, S.M.M. Coelho,P.J. Janse van Rensburg, P.N.M. Ngoepe. *Effects of 5.4 MeV alpha-particle irradiation on the electrical properties of nickel Schottky diodes on 4H–SiC* .Nuclear Instruments and Methods in Physics Research B 365 (2015) 264–268.

[16] E. Omotoso, W.E. Meyer, P.J. Janse van Rensburg, E. Igumbor, S.M. Tunhuma, P.N.M. Ngoepe, H.T. Danga, F.D. Auret,*The effects of high-energy proton irradiation on the electrical characteristics of Au/Ni/4H-SiC Schottky barrier diodes.* Nuclear Instruments and Methods in Physics Research B 409 (2017) 241–245.

[17] P. Vigneshwara Raja and N. V. L. Narasimha Murty *Thermally annealed gamma irradiated Ni/4H-SiC Schottky barrier diode characteristics* Journal of semiconductors 40 (2019) 022804.

[18] Indudhar Panduranga Vali, Pramoda Kumara Shetty, M. G. Mahesha, Mala N. Rao, Swayam Kesari.*Thermal neutron irradiation effects on structural and electrical properties of n-type 4H–SiC* Journal of Materials Science: Materials in Electronics (2020) 31:8496–8501.

[19] P. G. Baranov, B. Ya. Ber, I. V. Ilyin, A. N. Ionov, E. N. Mokhov, M. V. Muzafarova, M. A. Kaliteevskii, P. S. Kop'ev, A. K. Kaliteevskii, O. N. Godisov, and I. M. Lazebnik, *Peculiarities of neutron–transmutation phosphorous doping of Si 30 enriched SiC crystals: Electron paramagnetic resonance study*, J. Appl. Phys. 102 (2007) 063713.

[20] M. Kanaya, J. Takahashi, Y. Fujiwara, A. Moritani, *Controlled sublimation growth of single crystalline 4H–SiC and 6H–SiC and identification of polytypes by x–ray diffraction*, Appl. Phys. Lett. 58 (1991) 56–58.

[21] Z.C. Feng, A. Rohatgi, C.C. Tin, R. Hu, *Structural , Optical , and Surface Science Studies of 4H–SiC Epilayers Grown by Low Pressure Chemical Vapor Deposition*, J. Electron. Mater. 25 (1996) 917–923.

[22] H. Holloway, K. C. Hass, and M. A. Tamor, T. R. Anthony and W. F. Banholzer, *Isotopic dependence of the lattice constant of diamond*, Phy. Rev. B. 13 (1991) 7123–7126.

[23] S. Sorieul, J–M Costantini, L Gosmain, G Calas, J–J Grob and L Thome, S*tudy of damage in ion–irradiated α–SiC by optical spectroscopy*, J. Phys.: Condens. Matter 18 (2006) 8493–8502

[24] D. J. Brink, J. B. Malherbe, J. Camassel, *Neutron irradiation effects in SiC*, Nucl. Instr. Meth. Phys. Res. B 267 (2009) 2716–2718.

[25] S. Nakashima, T. Kitamura, T. Kato, K. Kojima, R. Kosugi, H. Okumura, H. Tsuchida, and M. Ito, *Determination of free carrier density in the low doping regime of 4H–SiC by Raman scattering*, Appl. Phys. Lett. 93, 121913 (2008).

[26] A.A. Lebedev, B.Y. Ber, N. V. Seredova, D.Y. Kazantsev, V. V. Kozlovski, *Radiation–stimulated photoluminescence in electron irradiated 4H–SiC*, J. Phys. D. Appl. Phys. 48 (2015) 485106.

[27] L. Liu, A. Liu, S. Bai, L. Lv, P. Jin and X. Ouyang, *Radiation Resistance of Silicon Carbide Schottky Diode Detectors in D–T Fusion Neutron Detection*, Sci. Rep. 7 (2017) 13376.

[28] E. V. Kalinina, N. A. Chuchvaga, E. V. Bogdanova, A. M. Strel'chuk, D. B. Shustov, M. V. Zamoryanskaya, and V. A. Skuratov, *Optical and Electrical Properties of 4H–SiC Irradiated with Xe Ions*, Semiconductors 48 (2014) 156–162.